In situ transmission electron microscope formation of a single-crystalline Bi film on an amorphous substrate

M. Neklyudova, C. Sabater, A. K. Erdamar, J. M. van Ruitenbeek, and H. W. Zandbergen

Citation: Appl. Phys. Lett. **110**, 103101 (2017);
View online: https://doi.org/10.1063/1.4977940
View Table of Contents: http://aip.scitation.org/toc/apl/110/10
Published by the American Institute of Physics

Articles you may be interested in

A niobium oxide-tantalum oxide selector-memristor self-aligned nanostack
Applied Physics Letters **110**, 103102 (2017); 10.1063/1.4977945

The role of nitrogen doping in ALD Ta_2O_5 and its influence on multilevel cell switching in RRAM
Applied Physics Letters **110**, 102902 (2017); 10.1063/1.4978033

GaN surface states investigated by electrochemical studies
Applied Physics Letters **110**, 101602 (2017); 10.1063/1.4977947

Dual-spacer nanojunctions exhibiting large current-perpendicular-to-plane giant magnetoresistance for ultrahigh density magnetic recording
Applied Physics Letters **110**, 102401 (2017); 10.1063/1.4977948

Contact resonance AFM to quantify the in-plane and out-of-plane loss tangents of polymers simultaneously
Applied Physics Letters **110**, 101902 (2017); 10.1063/1.4977936

Room temperature ferroelectricity in one-dimensional single chain molecular magnets $[\{M(\Delta)M(\Lambda)\}(ox)_2(phen)_2]_n$ (M = Fe and Mn)
Applied Physics Letters **110**, 102901 (2017); 10.1063/1.4977939

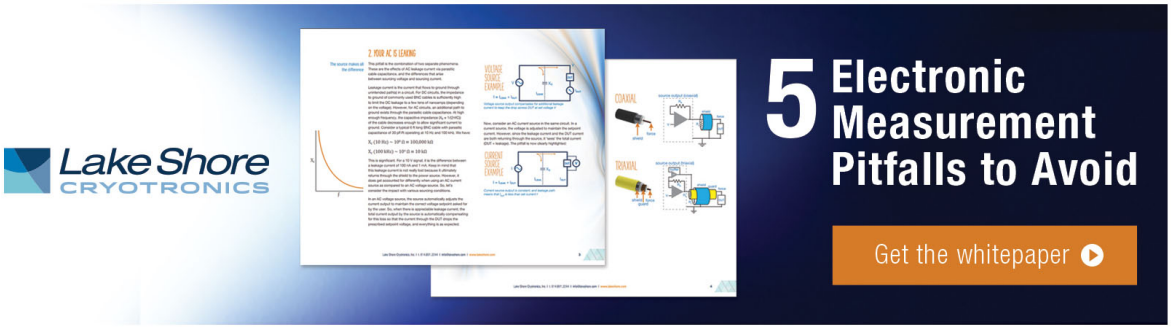

In situ transmission electron microscope formation of a single-crystalline Bi film on an amorphous substrate

M. Neklyudova,[1] C. Sabater,[2] A. K. Erdamar,[1] J. M. van Ruitenbeek,[2] and H. W. Zandbergen[1,a)]
[1]*Department of Quantum Nanoscience, Kavli Institute of Nanoscience, Delft University of Technology, Delft 2628CJ, The Netherlands*
[2]*Huygens-Kamerlingh Onnes Laboratory, Leiden Institute of Physics, Leiden University, Leiden 2333CA, The Netherlands*

(Received 19 December 2016; accepted 21 February 2017; published online 6 March 2017)

We have performed a range of *in situ* heating experiments of polycrystalline Bi films of 22–25 nm-thickness in a transmission electron microscope (TEM). This shows that it is possible to locally transform a polycrystalline thin film into a [111]-oriented single-crystalline film, whereby the unique feature is that the original thickness of the film is maintained, and the substrate used in our experiments is amorphous. The single-crystalline areas have been created by heating the Bi film to temperatures close to the melting temperature with additional heating by focusing of the electron beam (e-beam), which results in local melting of the film. The film does not collapse by dewetting, and upon subsequent cooling, the film transforms into a single-crystalline [111] oriented area. The observed phenomenon is attributed to the presence of a thin Bi-oxide layer on top of Bi film. We show that removal of the Bi-oxide layer by heating the film in a H_2 gas atmosphere results in changes in the Bi film thickness and dewetting upon *in situ* heating in the TEM. *Published by AIP Publishing.* [http://dx.doi.org/10.1063/1.4977940]

In recent years, interest in growth of thin Bi films has increased due to the unique properties of Bi in quasi-two dimensional geometry, such as quantum confinement effects[1] and very pronounced magnetoresistance.[2,3] It has been shown that low-dimensional Bi shows enhanced thermoelectric efficiency.[4] Moreover, recent theoretical[5,6] and experimental[7,8] studies indicate that a Bi (111)-bilayer is a topological insulator with protected electronic edge states.

The physical properties of thin metal films are strongly affected by imperfections such as grain boundaries (GBs). In the case of Bi, this effect is even more pronounced because the grain sizes are typically much smaller than the mean free path of the electrons. Therefore, much attention has been paid to fabricating Bi thin films on different substrates by various growth techniques, such as molecular beam epitaxy,[9,10] pulsed laser deposition,[11] thermal evaporation,[12] electrodeposition,[13] and dc sputtering[14] in order to enhance the quality of thin films and produce high-quality monocrystalline Bi films. Electrodeposition, thermal evaporation, and sputter deposition produce polycrystalline Bi films, the grain sizes of which depend on the deposition technique and substrate temperature, and the film quality can be improved by selecting optimal post-annealing conditions. An epitaxial growth of excellent quality can be obtained by molecular beam epitaxy.[9,10] However, to grow a single-crystalline Bi film with a low density of defects, this fabrication technique requires that single-crystalline substrates of high quality and small lattice mismatch be selected.

In this letter, we show that it is possible to transform a polycrystalline thin film of Bi into a [111]-oriented single-crystalline area, whereby the unique feature is that the original thickness of the film is maintained, and the substrate used in our experiments is amorphous. The single-crystalline area is created by heating the film close to the melting temperature (T_m) and using an e-beam to melt and, subsequently, cool the film to create a "sandwiched" single-crystalline area. We provide details about grain growth and the process of forming the liquid.

Polycrystalline Bi films with thicknesses of 22–25 nm were deposited by e-beam evaporation at room temperature (RT) with a slow deposition rate of 0.5 Å/s onto amorphous SiN at the back of the heating chips developed for *in situ* transmission electron microscope (TEM) heating experiments. The details of the heating chip fabrication for *in situ* TEM experiments are described elsewhere.[15] Before deposition of the Bi films, the heaters on the chips for *in situ* TEM experiments were calibrated by means of a pyrometer. The accuracy of the pyrometer calibration is only a few degrees, but the determination of temperature differences in our experiments is accurate to $<0.1\,^{\circ}C$ over a range of $10\,^{\circ}C$. In order to have the same offset, we used chips with the same resistances at RT, i.e. resistances of the same values including at least one decimal behind the point, which produce the same T_m within $0.1\,^{\circ}C$. In the rest of this paper, we give the temperature based on the pyrometer calibration and note that only the temperature change is very accurate. After deposition of Bi, the heating chip was placed into an in-house built TEM heating holder for *in situ* heating experiments. In order to limit Bi oxidation during exposure to air to the surface layers only, the chip was exposed to air for a maximum of 1 h before transfer into the TEM.

The *in situ* TEM heating experiments were performed using a FEI Titan microscope operated at 300 keV. Real-time TEM and diffraction pattern (DP) movies showing the

a)Electronic mail: H.W.Zandbergen@tudelft.nl

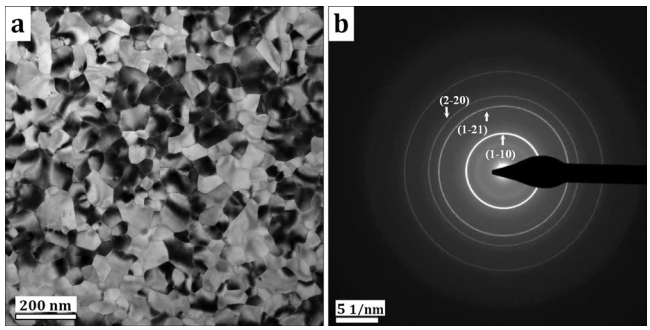

FIG. 1. (a) Bright-field TEM micrograph of the as-deposited Bi film. (b) Diffraction pattern of the as-deposited Bi film.

polycrystalline film transformation under *in situ* heating and e-beam bombardment were recorded with Camtasia screen recorder software from a FluCam screen and a Gatan camera. TEM images were acquired using the Gatan camera. A vacuum transfer MEMS-based TEM holder was used to conduct the bismuth oxide reduction experiment at elevated temperatures in a gas supply system outside the TEM and allowed to deliver a sample directly to the TEM column under vacuum without interaction with the ambient atmosphere.

A bright-field TEM micrograph of the as-deposited Bi film is shown in Figure 1(a). One can see that the Bi film is initially polycrystalline and consists of grains with well-defined grain boundaries (GBs). At RT, the grain sizes of the as-deposited 22 nm-thick film are observed to vary from 30 to 170 nm. A DP in Figure 1(b) taken from the area presented in Figure 1(a) shows that the initial as-deposited polycrystalline Bi film consists of [111]-oriented grains, rotated with respect to each other in the plane of the film. Note that the [111]-orientation of the grains is not imposed by the substrate because this is amorphous.

In situ TEM experiments were performed in order to investigate the polycrystalline Bi film behavior subjected to heating. The temperature of the heating chip was gradually increased until morphological changes were observed in the polycrystalline Bi films. Figure 2 shows TEM images corresponding to the same area of the Bi film acquired at different temperatures during this heating experiment. Figure 2(a) shows the as-deposited Bi film taken at RT. Figure 2(b) shows a TEM image recorded at 160 °C, where no significant changes are yet observed. At 243 °C in Figure 2(c), changes become visible in the shapes of some grains, and the positions of some GBs have changed. For example, grains G1 and G2 have become smaller at 243 °C, and the grain boundary (indicated as GB) related to G1 has become shorter. At 244.5 °C, Figure 2(d), a contrast change near triple junctions can be observed (circled): these areas become smooth and darker. Increasing the temperature further to 246 and 247.3 °C (Figures 2(e) and 2(f), respectively) leads to similar contrast changes along the GBs, and the widths of the smooth dark contrast areas at the triple junctions expand. Also, nearly each GB band has a dark contrast except low-

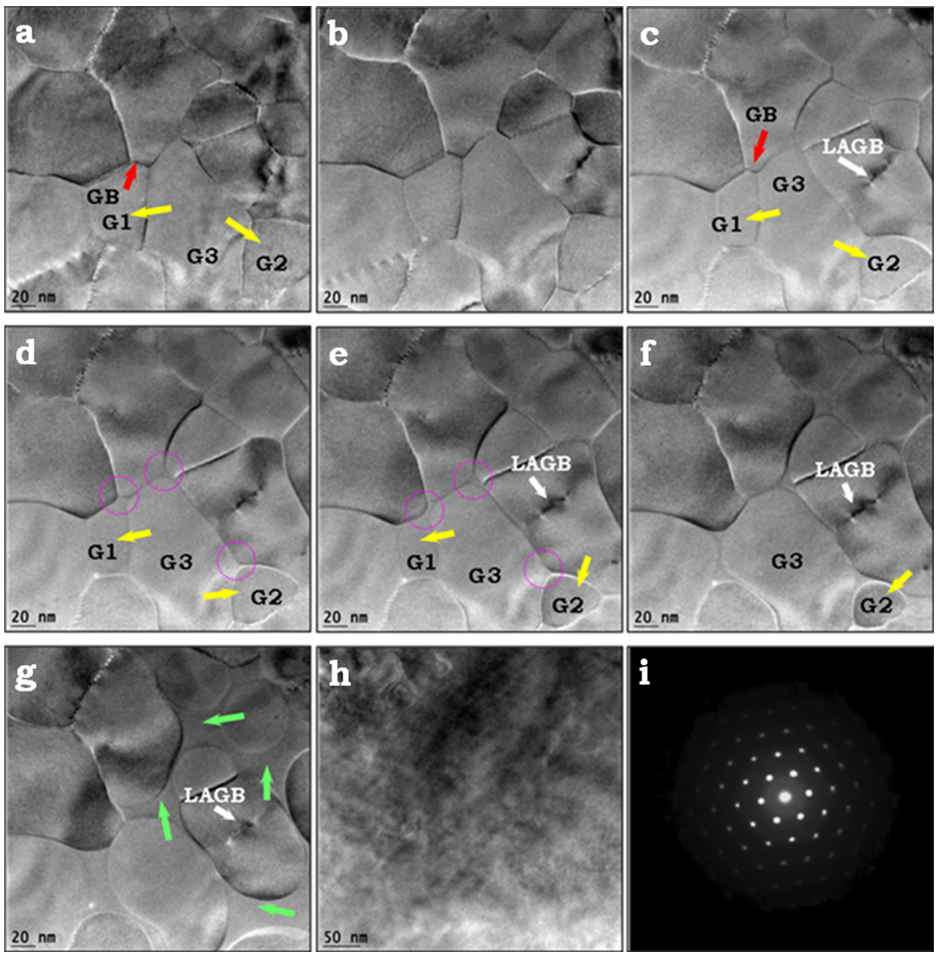

FIG. 2. TEM images showing the transformation of the Bi film area occurring at different temperatures during the heating experiment. (a) TEM image of as-deposited Bi film taken at RT. (b)–(g) Images of the same Bi film area as in (a) acquired at 160, 243, 244.5, 246, 247.3, and 248.6 °C, respectively. (h) TEM image acquired after cooling back to RT upon reaching 249.7 °C for the same field of view. (i) DP obtained from (h) and showing [111] zone axis of the single-crystal Bi film. Red arrows in (a) and (c) indicate the GBs that undergo changes upon heating. Yellow arrows in (a) and (c)–(f) indicate changes in the grains of interest. Purple circles indicate GB melting, and green arrows indicate the molten phase of Bi.

angle GBs (LAGBs), see Figures 2(e)–2(f), where LAGB is a GB between two adjoining grains with a small misorientation angle ($\theta < 11°$). This LAGB consists of a periodic array of dislocations and have a different contrast in TEM and can be easily distinguished.[16] At 248.6 °C in Figure 2(g), the grains are smaller and roundish in shape, and the dark GB bands have grown wider. With further increasing temperature, grain sizes decrease rapidly and most of them disappear, whereas the GB bands expand considerably. When raising the temperature to 249.7 °C, grains and GBs were no longer observable, and the contrast of the entire field of view becomes nearly homogeneous. At that moment, the temperature was immediately decreased to RT, and a TEM image and a DP (Figures 2(h) and 2(i), respectively) were taken from the same area. Both show that the area has been transformed into monocrystalline [111]-oriented Bi.

We attribute the growth of the smooth darker contrast areas at grain boundaries to GB melting.[17–19] The melting starts at triple junctions and, as the temperature rises, extends along the GBs, see Figures 2(e) and 2(f). As we increase the temperature, the width of this molten phase along the GBs increases, and the molten phase forms a connected network surrounding almost all the original grains except the ones that have disappeared, see Figure 2(g). We have verified that the phase growing at the grain boundaries has a diffuse DP, consistent with our interpretation as a liquid phase, see Figure S1 in supplementary material.

Remarkably—and in contrast to the common behavior in grain boundary melting—the thickness of the Bi film does not change significantly. This observation is exceptional because thin films are generally metastable in the as-deposited configuration and tend to dewet or agglomerate into islands upon heating even below a film's melting point.[20]

After the heating experiment, when we acquire a TEM image at low magnification, we find that only the region close to that irradiated by the e-beam (yellow circle) has been converted into a single crystal, see Figure 3(a). The segment of the film enclosed by the boundary marked in purple

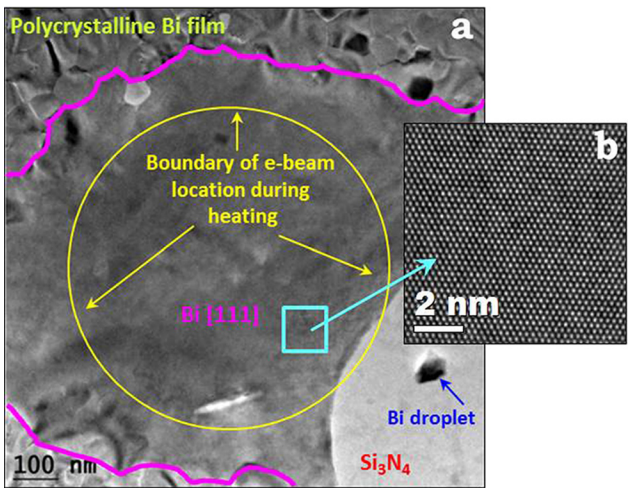

FIG. 3. (a) TEM image presenting an overview of the area transformed into a [111]-oriented Bi film under heating and e-beam irradiation. The e-beam position is indicated by the yellow circle. The border between the monocrystalline and the polycrystalline regions of the Bi film is shown in purple. (b) HRTEM image of the Bi film taken from the area indicated by the blue square in (a), demonstrating that the film has [111]-orientation.

is monocrystalline, while outside this segment, the film remained polycrystalline. This observation suggests that additional heating results from exposure to the e-beam during *in situ* Bi film heating. Figure 3(b) is a HRTEM image of the segment indicated by the blue square in Figure 3(a) and shows that Bi is single crystalline and [111]-orientated.

In Figure 3, no Bi film can be observed at the bottom right of the picture (only the SiN) which we attribute to a slight temperature gradient along the heating chip. As Bi is very sensitive to temperature variations near its T_m, a minor temperature gradient destabilizes the film and leads to dewetting and droplet formation. We have repeated the experiment for several independent Bi films, which uniformly confirm the local melting and crystallization behaviour. In most other experiments, the dewetting as in the lower edge in Figure 3 is not observed.

In order to investigate the role of e-beam, the heating experiment was repeated with the e-beam spread over a 5 μm area in diameter, to be compared with 600 nm diameter for the experiment shown in Figure 2. At 242–244 °C, we observe GB melting, and as we increase the temperature further to 250.5–251 °C, the Bi film collapses instantly and completely, and at RT, no Bi is visible in the 5 μm area. In the last image before this collapse, the structure is like that in Figure 2(g). Note that the collapse occurs at a temperature that is approximately 20° below the T_m of 271.4 °C for bulk Bi, which can be attributed to the melting-point suppression by size effects.[21–25]

With the e-beam focused to smaller diameters of 200 nm over several randomly chosen Bi film areas, we observed a similar behaviour as for 600 nm beam diameters, see Figure S2 in supplementary material. We found that the temperature required for melting all the grains in the field of view is slightly lower (0.1–0.2 °C) than in the previous experiment. This difference is probably due to the increase of e-beam current density by about a factor of 10 when the e-beam diameter is decreased from 600 nm to 200 nm. For an e-beam current of 5 nA and for 600 nm and 200 nm e-beam diameters, the doses are 1.1×10^5 and 10^6 electrons/nm^2 s, respectively. Egerton *et al.*[26] estimate the temperature rise in a carbon film with a low thermal conductivity $k \approx 1.6$ W m^{-1} K^{-1} which is comparable to that of Bi. For a 5 nA stationary probe and the e-beam diameters between 1 μm and 1 nm, the current density in the probe increases by a factor of 10^6, but the temperature increases only from 0.5 to 1.4 K. The electron-beam-induced heating in our experiments can be estimated fairly well because the melting of the illuminated area can be compared to that of the areas not exposed to the electron beam, or when a low beam intensity is used. According to our experiments, the estimation of e-beam-induced heating is about 0.8–1.5 °C. Note that the effect of electron-beam heating is strong for Bi compared to other metals because its thermal conductivity is low. We verified that the orientation of the e-beam does not influence the orientation and formation of the film, see Figure S3 in supplementary material.

The observed behavior of thin Bi films is quite different from that of other metal films on amorphous substrates at higher temperatures.[27–29] Normally, thin metal films are metastable as-deposited and, upon heating, tend to dewet and form islands due to surface-energy minimization, which can

happen even far below the T_m of the metal film while remaining in the solid state (e.g., an Au film dewetts already at 300 °C, whereas the T_m is 1050 °C). For Bi films, there is no dewetting at temperatures well below the T_m, and no significant change in thickness when the temperature is close to the T_m. We propose two main ingredients for the explanation of our observation of local transformation of a polycrystalline film to monocrystalline segments. First, the e-beam adds a small amount of local heating due to the low thermal conductivity of Bi. Second, the presence of a thin Bi-oxide layer formed during exposure the film to air after deposition stabilizes the film by reducing its surface energy. Note that the T_m of Bi-oxide is much higher than that of Bi.

The latter was tested by removing the oxide. A 22-nm-thick Bi film was deposited onto the back of a heating chip designed for vacuum transfer TEM holder, which enables gas treatment experiments at elevated temperatures in a gas supply system outside the TEM. It allows delivering a sample directly to the TEM column under vacuum or controlled gas conditions, thus preventing any interaction with the outside environment. The Bi-oxide reduction treatment was performed in a H_2 atmosphere with 1 bar of gas pressure at 60–80 °C for 1 h in a homemade gas supply system outside the TEM. Next, the reaction chamber was pumped to vacuum for 10 min, and the transfer holder was sealed to keep the sample in vacuum. Then, the holder was transferred to the TEM within 5 min without exposure to ambient air.

TEM images acquired upon heating this Bi film with the oxide layer removed are shown in Figure S4 in the supplementary material. Figure S4(a) (supplementary material) shows a TEM image of the starting morphology obtained at RT. Figure S4(b) (supplementary material) shows a TEM image obtained at 245.6 °C with a beam diameter of 1 μm for the same area as in Figure S4(a) (supplementary material). Apart from partial melting at GBs, Figure S4(b) (supplementary material) illustrates the fact that holes appear (white spots in the TEM image) in the film starting at triple junctions. At 246.7 °C and 248.4 °C (see Figures S4(c) and S4(d) (supplementary material), respectively), the holes expand and new holes are formed; all GBs have molten. At 249.3 °C, we observe that the molten (liquid) phase prevails in the field of view and that the number of holes has increased, see Figure S4(e) (supplementary material). A small increase in temperature to 249.5 °C causes the Bi film to collapse, see Figure S4(f) (supplementary material). Note that at every temperature step, the applied temperature is kept no longer than 1–2 s. Keeping the temperature close to the final T_m (so in this case 249.3 °C) would lead to further melting. Repeated observations of Bi films reduced in H_2 atmosphere confirmed that such films do not remain stable when heating up to the point of local melting, and do not produce crystalline areas. After reduction of the Bi-oxide layer on the Bi surface (see Figure S4 (supplementary material)), the film's behavior differs. For temperatures that were insufficient for all GBs to become molten, we observed the formation of several holes in the film, and these holes started to form in triple junctions. Moreover, the formation of holes is accompanied with a strong increase in mass-thickness contrast around the holes. On the other hand, an increase in mass-thickness contrast is clearly observed only around the formed holes.

The role of the oxide layer could lie in providing mechanical stability (the oxide layer acts as a scaffold) to the Bi film. When we cover the Bi before exposure to air (and thus no Bi-oxide layer is present) with Al_2O_3 by means of e-beam evaporation, we see the same behaviour as with the Bi-oxide layer. Bi-oxide layer is amorphous as well as the Al_2O_3 layer. We did not find any additional reflections in diffraction patterns which could belong to a crystalline Bi-oxide as reported elsewhere.[30] In case no Bi-oxide layer is present, we observe dewetting, but this only occurs when the temperature is close (about 2 K) to the T_m. It shows that the (111) plane of Bi is very stable, which is in agreement with the preferred cleavage along (111). Whereas the (111) surface of the Bi_{solid} has a low surface energy and thus prefers to be flat, the Bi_{liquid} can prefer a different shape because it has no anisotropy in its surface energy, and the shape will be defined by the various forces acting on the liquid phase: the interface energies of Bi_{solid}/Bi_{liquid}, SiN/Bi, and Bi/Bi-oxide, the Bi-oxide/vacuum. In case the Bi-oxide layer is monolayered or less, the oxide could act as a surfactant[31] and in this case, it is better to consider the system as consisting of three interfaces: Bi_{solid}/Bi_{liquid}, SiN/Bi, and surfactant stabilized Bi-oxide/vacuum. In the latter case, the liquid phase is expected to be like a droplet with a certain wetting angle and thus increasing in thickness towards the middle. We observe when the liquid phase grows that the thickness is roughly the same over the width of the liquid area, which favours an interpretation in terms of Bi-oxide acting as a scaffold rather than a surfactant. The presence of an oxide layer will also limit surface diffusion. In case there is a Bi-oxide layer on the Bi film, diffusion of Bi has to take place over the Bi-oxide surface or along the Bi-Bi-oxide interface. The stability of the Bi film up to the grain boundary melting indicates that both are hardly occurring.

In summary, our experiments indicate a possible route towards crystalline film growth for Bi on amorphous substrates, which has the great advantage that the films are not strained by lattice mismatch with the substrate. Bismuth has many unusual properties that combine in providing this path. First, the large anisotropy in surface energies results in a strongly textured film, where all grains have their ⟨111⟩ crystalline orientation perpendicular to the substrate surface. The low thermal conductivity permits gentle local heating by the e-beam of the TEM. Finally, the oxide formed at the surface acts to stabilize the film, thus allowing large area molten films to be (meta)stable for sufficiently long times permitting cool down and crystallization. This combination of properties results in a number of interesting observations. Our images show a clear evidence of grain boundary melting over extended width between the grains, without tendency to collapse. The final molten film in the field of view of the beam is stabilized by the oxide layer, and by the embedding Bi_{solid} film surrounding the beam region. Finally, during cool down, it appears that a single grain at the edge serves as a seed for the growth of the single crystal. This process must proceed very rapidly in order to explain the absence of multiple grains and grain boundaries in the final crystalline film.

It would be interesting to explore the use of the confinement by the substrate and a thin surface layer also for other materials, which would require a preferred orientation on an

amorphous substrate and a relatively low thermal conductivity.

See supplementary material for Figures S1–S4. Figure S1 shows the evolution of DP of Bi film upon heating. Figure S2 shows TEM images of the Bi-film area during heating with an additional irradiation of e-beam focused onto 200 nm diameter. Figure S3 shows that the orientation of the e-beam does not influence the orientation and formation of the film. Figure S4 presents TEM images acquired upon heating of Bi film with the removed oxide layer.

The authors gratefully acknowledge ERC Project No. NEMinTEM 267922 for financial support, and we thank J. W. M. Frenken, R. M. Tromp, and M. J. Rost for informative discussions.

[1]D. Gekhtamn, Z. B. Zhang, D. Adderton, M. S. Dresselhaus, and G. Dressehaus, Phys. Rev. Lett. **82**, 3887 (1999).
[2]S. Cho, Y. Kim, A. Freeman, G. Wong, J. Ketterson, L. Olafsen, I. Vurgaftman, J. Meyer, and C. Hoffman, Appl. Phys. Lett. **79**, 3651 (2001).
[3]C. L. Chien, F. Y. Yang, K. Liu, D. H. Reich, and P. C. Searson, J. Appl. Phys. **87**, 4659 (2000).
[4]A. L. Prieto, M. M. Gonzalez, J. Keyani, R. Gronsky, T. Sands, and A. M. Stacy, J. Am. Chem. Soc. **125**, 2388 (2003).
[5]S. Murakami, Phys. Rev. Lett. **97**, 236805 (2006).
[6]M. Wada, S. Murakami, F. Freimuth, and G. Bihlmayer, Phys. Rev. B: Condens. Matter Mater. Phys. **83**, 121310 (2011).
[7]C. Sabater, D. Gosálbez-Martínez, J. Fernández-Rossier, J. G. Rodrigo, C. Untiedt, and J. J. Palacios, Phys. Rev. Lett. **110**, 176802 (2013).
[8]T. Hirahara, G. Bihlmayer, Y. Sakamoto, M. Yamada, H. Miyazaki, S. Kimura, S. Blugel, and S. Hasegawa, Phys. Rev. Lett. **107**, 166801 (2011).
[9]M. Chen, J.-P. Peng, H.-M. Zhang, L.-L. Wang, K. He, X.-C. Ma, and Q.-K. Xue, Appl. Phys. Lett. **101**, 081603 (2012).
[10]K. Ishioka and M. Kitajima, Phys. Rev. B **91**, 125431 (2015).
[11]M. O. Boffoué, B. Lenoir, H. Scherrer, and A. Dauscher, Thin Solid Films **322**, 132 (1988).
[12]L. Kumari, S.-J. Lin, J.-H. Lin, Y.-R. Ma, P.-C. Lee, and Y. Liou, Appl. Surf. Sci. **253**, 5931 (2007).
[13]F. Y. Yang, K. Liu, C. L. Chien, and P. C. Searson, Phys. Rev. Lett. **82**, 3328 (1999).
[14]J.-H. Hsu, Y.-S. Sun, H.-X. Wang, P. C. Kuo, T.-H. Hsieh, and C.-T. Liang, J. Magn. Mater. **272**, 1769 (2004).
[15]M. A. van Huis, N. P. Young, G. Pandraud, J. F. Creemer, D. Vanmaekelbergh, A. I. Kirkland, and H. W. Zandbergen, Adv. Mater. **21**, 4992 (2009).
[16]P. Lejček, *Springer Series in Materials Science* (Springer, 2010), Vol. 136, p. 5.
[17]Q. S. Mei and K. Lu, Prog. Mater. Sci. **52**, 1175 (2007).
[18]A. M. Alsayed, M. F. Islam, J. Zhang, P. J. Collings, and A. G. Yodh, Science **309**, 1207 (2005).
[19]P. N. Pursey, Science **309**, 1198 (2005).
[20]C. V. Thompson, Annu. Rev. Mater. Res. **42**, 399 (2012).
[21]N. T. Gladkikh, S. I. Bogatyrenko, A. P. Kryshtal, and R. Anton, Appl. Surf. Sci. **219**, 338 (2003).
[22]J. Sun and S. L. Simon, Thermochim. Acta **463**, 32 (2007).
[23]A. F. Lopeandia and J. Rodriguez-Viejo, Thermochim. Acta **461**, 82 (2007).
[24]M. Takagi, J. Phys. Soc. Jpn. **9**, 359 (1954).
[25]S. L. Lai, J. Y. Guo, V. Petrova, G. Rammath, and L. H. Allen, Phys. Rev. Lett. **77**, 99 (1996).
[26]R. F. Egerton, P. Li, and M. Malac, Micron **35**, 399 (2004).
[27]C. M. Muller and R. Spolenak, Acta Mater. **58**, 6035 (2010).
[28]O. Kovalenko, J. R. Greer, and E. Rabkin, Acta Mater. **61**, 3148 (2013).
[29]F. Niekiel, P. Spiecker, S. M. Kraschewski, B. Butz, and E. Spiecker, Acta Mater. **90**, 118 (2015).
[30]K. J. Stevens, B. Ingham, M. F. Toney, S. A. Brown, J. Partridge, A. Ayesh, and F. Natali, Acta Cryst. B **63**, 569 (2007).
[31]D. Kandel and E. Kaxiras, Solid State Phys. **54**, 219 (2000).